Srinivasan *et al. J Wireless Com Network (2020) 2020:238*
https://doi.org/10.1186/s13638-020-01840-z

EURASIP Journal on Wireless Communications and Networking

RESEARCH Open Access

Enhanced interpolation-based interference rejection combining for black-space cognitive radio in time-varying channels

Sudharsan Srinivasan*, Sener Dikmese and Markku Renfors

*Correspondence:
sudharsan.srinivasan@tuni.fi
Electrical Engineering, Faculty of Information and Communication Sciences, Tampere University, Tampere, Finland

Abstract

In this paper, we investigate multi-antenna interference rejection combing (IRC)-based black-space cognitive radio (BS-CR) operation in time-varying channels. The idea of BS-CR is to transmit secondary user (SU) signal in the same frequency band with the primary user (PU) such that SU's power spectral density is clearly below that of the PU, and no significant interference is inflicted on the PU receivers. We explore the effects of interpolation and mobility on the novel blind IRC technique which allows such operation mode for effective reuse of the PU spectrum for relatively short-distance CR communication. We assume that both the PU system and the BS-CR use orthogonal frequency division multiplexing (OFDM) waveforms with common numerology. In this case, the PU interference on the BS-CR signal is strictly flat-fading at subcarrier level. Sample covariance matrix-based IRC adaptation is applied during silent gaps in CR operation. We evaluate the effect of the gap length on the link performance, using known PU channel-based interference covariance estimation as reference. We also propose an interpolation-based scheme for tracking the spatial covariance in time-varying channels, demonstrating significantly improved robustness compared to the earlier scheme. The performance of the proposed IRC scheme is tested considering terrestrial digital TV broadcasting (DVB-T) as the primary service. Also joint PU and co-channel CR interference cancellation is included in the study. The resulting interference suppression capability is evaluated with different PU interference power levels, silent gap durations, data block lengths, and CR device mobilities.

Keywords: Black-space cognitive radio, Underlay CR, IRC, Interference rejection combining, Multi-antenna system, Receiver diversity, Mobility, OFDM, DVB-T

1 Introduction

Cognitive radios (CRs) are intended to operate in radio environments with a high level of interference and, simultaneously, produce negligible interference to the primary users (PUs) [1–3]. CR studies in the past have been focusing on opportunistic white-space scenarios where the unused spectrum is dynamically identified and used. Also underlay CR operation has received some attention. Here the idea is to transmit in wide frequency band with low power-spectral density, typically using spread-spectrum techniques [4]. Black-space CR (BS-CR), where a CR deliberately transmits simultaneously along the

primary signal in the same time–frequency resources without causing objectionable interference, has received limited attention [5–8]. An underlay CR is ignorant about the existence of PUs in its frequency band. Commonly, it uses very low power spectral density and wide bandwidth, such that it does not cause interference to the PU transmission under any conditions [4]. BS-CR adapts its waveform and signal parameters depending on the ongoing PU transmissions and uses advanced signal processing techniques on the receiver side to facilitate low signal-to-interference ratio (SIR) at the receiver. BS-CR systems effectively reuse the spectrum for communication over short distances. It can operate with limited spectrum resources and can be used without any additional spectrum sensing.

As discussed in our previous papers [9, 10], one of the major requirements for CR operation is to minimize the interference to the primary transmission system. In BS-CR, this is reached by setting the CR transmission power at a small-enough level. The most important factor that enables such a radio system is that stronger interference is easier to deal with as compared to weaker interference [11], if proper interference cancellation techniques are utilized. Previous studies from information theory provide theoretically achievable bounds for such cognitive radios [12]. Multi-antenna systems allow for spatiotemporal signal processing, which do not only improve the detection capability of the receiver but also improve performance in fading multipath channels with interference. Various methods of interference cancellation can be found in [13, 14-18] and the references therein. All other detection algorithms except the multi-user detector perform sub-optimally [13].

The interference rejection combining (IRC) receivers have the significant advantage in comparison with the other receivers in multi-user scenarios that they do not need detailed information about the interfering signals, such as modulation order and radio channel propagation characteristics. For CR scenarios, IRC receivers in general are simple and desirable compared to optimum detectors. IRC techniques are widely applied for mitigating co-channel interference, e.g., in cellular mobile radio systems like LTE-A [19]. The use of multiple antennas in CRs has been studied earlier, e.g., in [18]. Our initial study on this topic in highly simplified scenario with suboptimal algorithms was in [20], but to the best of our knowledge, IRC has not been applied to BS-CR (or underlay CR) elsewhere. In this current study, we develop the ideas that we presented in [9] under more practical situations and study the performance of our algorithms in more details. Notably, the scheme studied in [9] was found to be very sensitive to mobility, because its performance is critically affected by errors in spatial covariance estimation. In this work, we extent our previous studies on the effects of mobility and propose a scheme to improve the quality of the covariance estimation with time-varying channels using interpolation between sample covariance-based estimates.

In this paper, we consider BS-CR operation in the terrestrial TV frequency band, utilizing a channel with an ongoing relatively strong TV transmission. The PU is assumed to be active continuously. If the TV channel becomes inactive, this can be easily detected by each of the CR stations in the reception mode. Then the CR system may, for example, continue operation as a spectrum sensing-based CR system. In our case study, we focus on a scenario with multi-antenna CR receiver having IRC capability to mitigate co-channel interference generated by a single PU transmitter and multiple independent

(uncoordinated) CR systems. Generally, interference covariance matrix estimation is a key element of IRC schemes. For this purpose, we propose to use sample covariance calculated from the received signal during silent periods (gaps) in the target CR transmission. More specifically, the contributions of this paper are listed below:

- This paper extends and refines our earlier studies in papers [9, 10] on IRC schemes operating under severe interference conditions, with applications in BS-CR.
- Under such conditions, the direct estimation of the target CR channel is not possible. After estimating the interference covariance matrix during silent gaps in the target CR transmission, our scheme extracts from the received signal a set of signals which span the interference-free subspace in spatial domain. The weight vector for the target CR signal is based on pilot-based target channel estimation in this subspace.
- In BS-CR scenarios, the target CR link performance is very sensitive to the quality of the interference covariance estimate. Therefore, we propose to use linear interpolation of the interference covariance matrix to track the channel variations between consecutive interference covariance estimates, i.e., consecutive silent gaps.
- Our case study focuses on a TV whitespace (TVWS) scenario. We consider a multi-antenna CR receiver having IRC capability to mitigate co-channel interference generated by a single PU transmitter and multiple independent (uncoordinated) CR systems. The performance of such a system under different interference levels, mobilities, silent gap lengths, frame structures, and modulation orders is studied, and the improved robustness obtained through covariance interpolation is highlighted

The rest of the paper is organized as follows: In Sect. 2, the BS-SC scenario and proposed IRC scheme are first explained. Then also the connections between the signal-to-interference ratios (SIRs) at the PU and CR receivers are analyzed based on the channel losses of the target and interference links. The system model and IRC process are formulated in Sect. 3. Section 4 presents the simulation setup and performance evaluation results. Finally, concluding remarks are presented in Sect. 5.

2 IRC-based black-space cognitive radio scenario—scenario and methods

In our basic scenario, illustrated in Fig. 1, we consider a CR receiver using multiple antennas to receive data from a single-antenna cognitive transmitter. The details of the receiver signal processing indicated in the figure are explained in Sect. 3. The CR operates within the frequency band of the PU, and the PU power spectral density (PSD) is very high in comparison with that of the CR. The primary transmission is assumed to be always present when the CR system is operating. The primary transmitter generates a lot of interference to the CR transmission, which operates closer to the noise floor of the primary receiver, and due to this, the primary communication link is protected. We consider frequency reuse over relatively small distances, such as an indoor CR system. The multi-antenna configuration studied here is that of single-input multiple output (SIMO). Other configurations, involving also transmit diversity in the CR link, are also possible, but they are left as a topic for future studies.

Here the PU is a cyclic prefix orthogonal frequency division multiplexing (CP-OFDM)-based DVB-T system [21]. The CR system is also an OFDM-based multi-carrier

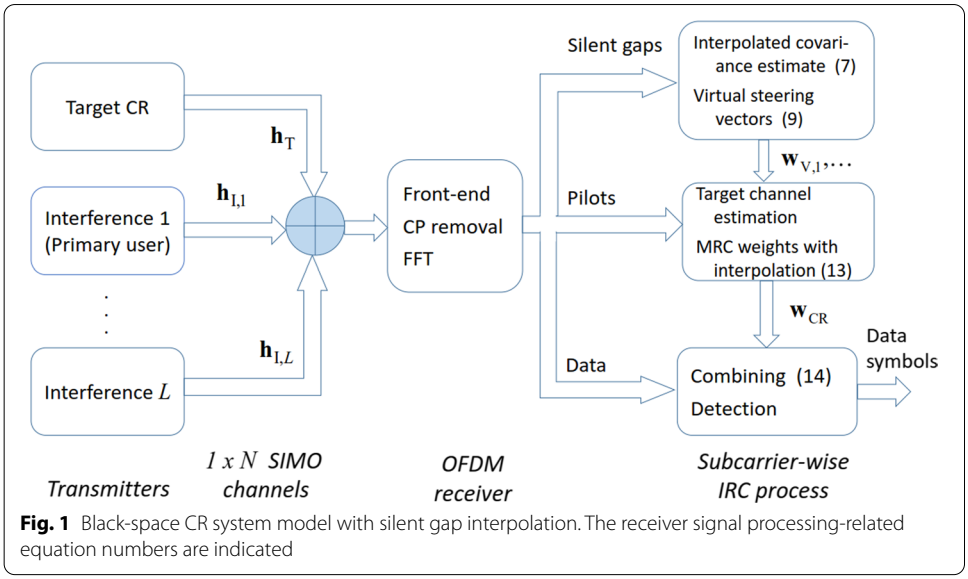

Fig. 1 Black-space CR system model with silent gap interpolation. The receiver signal processing-related equation numbers are indicated

system using the same subcarrier spacing and CP length as the primary system. Thus, it has the same overall symbol duration. The CR receiver is assumed to be synchronized to the primary system in frequency and in quasi-synchronous manner also in time. The CP length is assumed to be sufficient to absorb the channel delay spread together with the residual timing offsets between the two systems observed at the CR receiver. Consequently, the subcarrier-level flat-fading circular convolution model for spatiotemporal channel effects applies to the target CR signal and to the PU interference signal as well. Then the IRC process can be applied individually for each subcarrier. Since the CR receiver observes the PU signal at very high SINR level, synchronization task is not particularly difficult and low-complexity algorithms can be utilized. Considering short-range CR scenarios, the delay spread of the CR channel has a minor effect on the overall channel delay spread to be handled in the time alignment of the two systems. The same applies to the possible significant co-channel CR interferers, which are assumed to be at relatively short distance from the target CR system.

Basically, if all target and interfering CR stations are synchronized to their respective observed PU signals, they are also synchronized with each other in the quasi-synchronous manner, such that all multi-path components of all signals are within the CP length.

In addition to these, we assume that the secondary user experiences slow (e.g., pedestrian) mobility effects, due to either the mobility of devices or people moving around them. The effects of mobility on the CR system performance are evaluated in this study.

Both the primary and the CR systems use QAM subcarrier modulation, but usually with different modulation orders. The frame structures and pilot patterns of the PU and CR are independent. The received CR signal consists of contributions from the desired CR communication signal, co-channel CR interferers, and the primary transmission signal, the latter one constituting the dominating interference. Our proposed scheme includes two phases in the CR system operation as described in our previous work [9]. The spatial characteristics of the PU interference are modeled using multi-antenna sample covariance matrix, which is estimated during silent gaps in the target

CR transmission, independently for each active subcarrier. No explicit channel estimation of the PU channel is required. The CR channel is estimated from the partial IRC signals, from which the PU and other CR interferences have been effectively suppressed.

2.1 Methods

In this work, we study how channel fading with mobility affects the performance in the scenario described above. We consider adaptation of the IRC process using interpolation of the sample covariance matrices between the silent gaps. This is expected to improve the performance, allowing to increase the data block length between silent gaps, thus reducing the related overhead in throughput. The main elements of the scheme, covariance estimation and interpolation, IRC process, channel estimation [22], and MRC-based detection are formulated mathematically. Numerical performance results are obtained through Monte Carlo simulations based on a developed Matlab script, using a semi-analytical model based on PU channel knowledge as reference.

2.2 SIR analysis

Key parameters in BS-CR operation are the SIRs at the CR receiver and PU receiver. In the basic scenario with PU interference only, the SIRs can be expressed in dB units as follows:

$$SIR_{\mathrm{CR}} = (P_{\mathrm{CR}} - L_{\mathrm{CR-CR}}) - (P_{\mathrm{PU}} - L_{\mathrm{PU-CR}}) \tag{1}$$

$$SIR_{\mathrm{PU}} = (P_{\mathrm{PU}} - L_{\mathrm{PU-PU}}) - (P_{\mathrm{CR}} - L_{\mathrm{CR-PU}}), \tag{2}$$

where P_{CR} and P_{PU} are the transmission powers of CR and PU, respectively, in dBm units, while the other parameters are transmission losses in dB units of relevant transmission links. The first part of the subscript indicates the transmitter, and second part the receiver of the corresponding link. From these equations, it is easy to derive the maximum SIR of the CR receiver in terms of the minimum SIR of a PU receiver, $SIR_{\mathrm{PU,min}}$:

$$SIR_{\mathrm{CR,max}} = (L_{\mathrm{CR-PU}} - L_{\mathrm{CR-CR}}) + (L_{\mathrm{PU-CR}} - L_{\mathrm{PU-PU}}) - SIR_{\mathrm{PU,min}}. \tag{3}$$

The maximum SIR of the CR link depends on the differences of the channel losses from CR TX to both receivers and from PU TX to both receivers. For example, if the losses of the main links (CR-CR and PU–PU) are equal to the losses of the corresponding interfering links (CR-PU and PU-CR), then the CR RX would be able to operate with the SIR of $-SIR_{\mathrm{PU,min}}$. If the main link losses are lower than those of the interference links, the $SIR_{\mathrm{CR,max}}$ would be higher. The critical cases are:

1. If the losses of the main links (CR-CR and PU–PU) are much higher than the losses of the corresponding interfering links (CR-PU and PU-CR), then SIR of the CR receiver may be limited by the minimum acceptable PU SIR to a highly negative value. Then the SIR of the CR receiver may be limited to a highly negative value by the maximum transmit power of the CR device, which could be much lower than that of the PU transmitter.
2. If the PU transmitter is very close to the (short-range) CR system, then

$$SIR_{\mathrm{CR,max}} = P_{\mathrm{CR,max}} - L_{\mathrm{CR-CR}} - (P_{\mathrm{PU}} - L_{\mathrm{PU-CR}}). \tag{4}$$

Then the SIR of the CR receiver may be limited to a highly negative value by the maximum transmit power of the CR device, which could be much lower than that of the PU transmitter.

In both cases, the performance of the IRC scheme would be limited by the RF imperfections (e.g., receiver nonlinearity effects) in practice. The latter limitation appears especially in the TVWS application, but in rather limited geographical regions. Considering the first kind of limitation in the worst-case scenario, one should consider the hidden node margin (typically around 25–30 dB in the TVWS case [23] for the loss difference from PU ($L_{\mathrm{PU-PU}} - L_{\mathrm{PU-CR}}$), which would lead to very low SIR for the CR TX, unless the loss from the CR to the PU RX can be guaranteed to be much lower than that of the CR link. On the other hand, in short-range CR communication, especially if PU receivers use directive (possibly roof-top) antennas, the mentioned case where the SIR of CR RX is no less than $-SIR_{\mathrm{PU,min}}$ should be possible.

Generally, the CR TX should have knowledge of the link losses in order to maximize its transmission power while not causing excessive interference to the PU link. This paper focuses on the physical layer capabilities of IRC-based BS-CR, and detailed procedures for controlling the CR operation remain as a topic for future studies. One possible way to enhance BS-CR operation would be cooperative spectrum sensing of CR devices to reliably estimate the PU power level in the CR operation region.

3 IRC for black-space cognitive radio

Based on the OFDM model mentioned above, subcarrier-wise detection is considered with flat-fading channel coefficients to get rid of the challenge of frequency selectivity in the IRC process.

In the SIMO configuration, the CR is assumed to have N receiver antennas and L different interference sources are assumed. Based on this model, the signal received by the CR can be formulated for each active subcarrier as follows:

$$\mathbf{r} = \mathbf{h}_{\mathrm{T}} x_{\mathrm{T}} + \sum_{l=1}^{L} \mathbf{h}_{\mathrm{I},l} x_{\mathrm{I},l} + \boldsymbol{\eta}. \tag{4}$$

Here x_T is a transmitted subcarrier symbol and $\mathbf{h}_{\mathrm{T}} = [h_{\mathrm{T},1}, h_{\mathrm{T},2}, \ldots, h_{\mathrm{T},N}]^{\mathrm{T}}$ is the target channel vector with N receiver antennas in the CR, $x_{I,l}$ is the lth interfering signal, and $\mathbf{h}_{\mathrm{I,l}} = \left[h_{\mathrm{I,l},1}, h_{\mathrm{I,l},2}, \ldots, h_{\mathrm{I,l},N}\right]^{\mathrm{T}}$ is the channel vector for the lth interferer. The channel vectors consist of the complex channel gains from the corresponding transmit antenna to nth antenna of the CR receiver. Finally, $\boldsymbol{\eta}$ is the additive white Gaussian noise (AWGN) vector. In this generic system model, it is assumed that the PU is the dominant interferer, and the other interference sources are other CR systems introducing co-channel interference at relatively low power level.

3.1 Covariance matrix estimation

As it is illustrated in Fig. 1, the interference minimizing IRC weights are obtained during a silent period in the target CR transmission, while the co-channel interference sources are active. Due to that, Eq. (4) can be modified during silent gaps of CR operation as

$$\hat{\mathbf{r}} = \sum_{l=1}^{L} \mathbf{h}_{\mathrm{I},l} x_{I,l} + \boldsymbol{\eta}. \tag{5}$$

Here it is assumed that only interferences and noise are present during the silent period in the signal $\hat{\mathbf{r}}$ observed by the CR. Linear combiner is used for the signals from different antennas with a weight process in detection as follows:

$$y = \mathbf{w}^{\mathrm{H}}\mathbf{r}, \tag{6}$$

where y is the detected signal, $\mathbf{w}$ is the weight vector with N elements, and superscript H denotes the Hermitian (complex-conjugate transpose).

Determining the optimum weight values is an optimization problem which can be solved with the linear minimum mean-squared error (LMMSE) criterion [21, 22] that aims to minimize the mean-squared error with respect to the target signal x_T,

$$J = E\left[\left|x_{\mathrm{T}} - \mathbf{w}^{\mathrm{H}}\mathbf{r}\right|^2\right]. \tag{7}$$

When knowledge of the covariance matrix is available, IRC can be applied. Two cases are considered below: (i) calculating interference covariance from known channel coefficients and (ii) sample covariance-based approaches.

3.2 Perfect channel information case

The deterministic known channel case (with perfect channel information) is considered as the theoretical bound in this study. Assuming that the channel vectors form the interferers are perfectly known, the noise plus interference covariance matrix can be calculated for each subcarrier as

$$\boldsymbol{\Sigma}_{\mathrm{NI}} = \sum_{l=1}^{L} P_l \mathbf{h}_{\mathrm{I},l} \mathbf{h}_{\mathrm{I},l}^{\mathrm{H}} + P_{\mathrm{N}}\mathbf{I}, \tag{8}$$

where P_l is the variance of interferer l at the transmitter, P_{N} is the noise variance that can be obtained from the SNR, and $\mathbf{I}$ is the identity matrix of size NxN. Assuming that also the channel vector for the target signal is known and the target and interfering signals are Gaussian and statistically independent from each other, the conventional LMMSE solution for the weight vector is [15]

$$\mathbf{w} = \boldsymbol{\Sigma}_{\mathrm{NI}}^{-1}\mathbf{h}_{\mathrm{T}}\left(\mathbf{h}_{\mathrm{T}}^{\mathrm{H}}\boldsymbol{\Sigma}_{\mathrm{NI}}^{-1}\mathbf{h}_{\mathrm{T}} + \frac{1}{P_{\mathrm{T}}}\right)^{-1} \tag{9}$$

where P_{T} is the target CR transmitters signal power and unit noise variance is assumed.

In the BS-CR scenario with a single dominant interferer, the estimation of the PU channel is relatively straightforward if the CR knows PUs pilot structure. However, in the case of multiple interferers, the channel vectors of all interferers should be estimated, which becomes quite challenging. Furthermore, the target channel cannot be estimated before the interference cancellation. Therefore, the perfect channel information case serves mainly as an ideal reference in performance comparisons, as will be seen in Sect. 4.

3.3 Sample covariance-based case without PU channel information

The IRC process starts from interference covariance matrix estimation during silent gaps in the receiver. It is difficult to have the perfect channel state information on the CR receiver side. Alternatively, the joint interference and noise covariance matrix can be estimated for each subcarrier by the sample covariance matrix of the corresponding received subcarrier signal (after CP removal and FFT) in the absence of the target transmission, i.e., during the silent gaps as.

$$\overline{\Sigma}_{\mathrm{NI}} = \frac{1}{M} \sum_{m=1}^{M} \mathbf{r}(m)\mathbf{r}(m)^{H}. \tag{10}$$

Here m is the OFDM symbol index and M is the observation length in subcarrier samples, which is chosen equal to the length of the silent gap.

3.4 Linear interpolation for interference covariance tracking with mobility

Regarding the mobility aspects, there are significant differences in the effects of PU transmitter mobility, CR transmitter mobility, and CR receiver mobility. If the PU transmitter is stationery and CR receiver is stationary, the mobility of CR transmitter is easier to handle, because the dominating PU interference is stationary, and the variations in the noise and interference covariance matrix are only due to the co-channel CR interferes. However, even in this case, radio environment of the CR receiver may vary due to movement of people or vehicles nearby. Therefore, some tolerance to mobility is required also in such scenarios, at least with pedestrian mobilities. The mobility of PU transmitter or CR receiver makes the dominant interference time-varying, and in the BS-CR scenario, the CR link performance is very sensitive to quality of the PU interference covariance matrix estimate. Therefore, it is important to investigate these mobility effects and consider enhanced schemes for tracking the interference covariance with mobility.

While considering the sample covariance-based approach, increased observation (silent gap) length gives better PU interference covariance estimate in the stationary case or with low mobility. However, the channel variations during the silent gap affect critically the quality of the PU interference covariance matrix. Therefore, the optimum length of the silent gap (i.e., observation length) depends on the mobility, i.e., Doppler spread. Then we apply linear interpolation for the covariance matrix elements when calculating the weight vectors for the data symbols between two consecutive silent gaps.

There are two key parameters in this process, the silent gap length and the data block length between two consecutive gaps. Increasing the gap length improves the performance with low mobility but degrades the performance with higher mobility and

increases the overhead in throughput. Increasing the data block length increases the throughput but degrades the performance with mobility. These tradeoffs are investigated through simulations in Sect. 4 of this paper.

3.5 IRC process

As indicated in the model shown in Fig. 1, the CR channel cannot be estimated before the step of the interference cancellation, and the optimal steering vector for IRC cannot be directly calculated. Here we develop an IRC scheme which utilizes N orthogonal virtual steering vectors in the receiver's internal channel estimation process, which is based on pilot symbol structures typically used in OFDM systems. Actually, N-L vectors would be enough since IRC consumes L degrees of freedom. But this way the model is more straightforward and the IRC process is generic and robust since there is no need to estimate the number of interferers. Without loss of generality and for simplified computations, the following unit vectors are applied as the virtual steering vectors,

$$\begin{aligned}
&\mathbf{h}_{\mathrm{V},1} = [1,0,0,0,\ldots,0]^T \\
&\mathbf{h}_{\mathrm{V},2} = [0,1,0,0,\ldots,0]^T \\
&\ldots \\
&\mathbf{h}_{\mathrm{V},N} = [0,0,0,0,\ldots,1]^T.
\end{aligned} \tag{11}$$

Basically, the weight vectors obtained when applying the virtual steering vectors for $\mathbf{w}$ in Eq. (9) span the interference-free subspace in spatial domain. Assuming that the interference covariance is correctly estimated, using any linear combination $\mathbf{h}$ of these vectors instead of $\mathbf{h}_{\mathrm{T}}$ in (9) provides interference cancellation and maximizes signal power for the spatial CR channel h. The following process finds the combination of the virtual steering vectors for the actual target signal by first estimating the spatial channel vectors corresponding to the different virtual steering vectors. The obtained weight vectors are as follows:

$$\mathbf{w}_{\mathrm{V},n} = \overline{\Sigma}_{\mathrm{NI}}^{-1}\mathbf{h}_{\mathrm{V},n}. \tag{12}$$

It should be noted that the denominator of Eq. (9) is a complex scaling coefficient, which will be included in the MRC weights.

3.6 Target channel estimation with linear interpolation and MRC combining

In the second stage, data symbols of the CR link are transmitted together with the training/pilot symbols. While receiving pilot symbols, the weighted output signals corresponding to each virtual steering vector are calculated as

$$y_n = \mathbf{w}_{\mathrm{V},n}^{\mathrm{H}}\mathbf{r}, \quad n = 1,2,\ldots,N. \tag{13}$$

The IRC process cancels the interference from all of the weighted output signals, y_n corresponding to different virtual steering vectors. For each subcarrier, the N channel coefficients for each of the weighted output signals can be estimated using the pilot symbols as follows:

$$\hat{g}_{\mathrm{V},n} = \frac{y_n}{p} = \frac{\mathbf{w}_{\mathrm{V},n}^{\mathrm{H}} \cdot \mathbf{r}}{p},\ n = 1, 2, \ldots, N, \tag{15}$$

where p is the transmitted pilot symbol value.

3.7 Linear interpolation for channel estimation

In the traditional pilot-based channel estimation process, it is required to use efficient interpolation techniques, such as Wiener interpolation, based on the channel information at pilot sub-carrier symbols. For simplicity and to avoid excessive received signal buffering over high number of OFDM symbols, we apply linear interpolation. The performance of linear interpolation technique is better than the piecewise-constant interpolation methods [24, 25]. In the simulation studies of Sect. 4, a basic training symbol scheme is assumed where training symbols contain pilots in all active subcarriers, and the interpolation is done in time domain only, between two consecutive pilots in each subcarrier.

The MRC weights for a data symbol are then calculated as

$$\mathbf{w}_{\mathrm{MRC}} = \frac{[\overline{g}_{\mathrm{V},1}, \overline{g}_{\mathrm{V},2}, \ldots, \overline{g}_{\mathrm{V},N}]^{\mathrm{T}}}{\sqrt{\sum_{n=1}^{N} \left|\overline{g}_{\mathrm{V},n}\right|^2}}, \tag{16}$$

where $\overline{g}_{\mathrm{V},n}$, $n = 1, \ldots, N$, denote the corresponding interpolated channel estimates. Generally, the interpolated channel estimates are different for each subcarrier in each OFDM symbol. For simplicity, the subcarrier and OFDM symbol indexes are not included in the notation above. Then the interpolated channel estimates are given as

$$\overline{g}_{\mathrm{V},n}^{(k,m)} = \left(m - S_{\mathrm{p}}\right) \cdot \hat{g}_{\mathrm{V},n}^{(k,S_{\mathrm{p}})} + \left(S_{\mathrm{f}} - m\right) \cdot \hat{g}_{\mathrm{V},n}^{(k,S_{\mathrm{f}})} \tag{17}$$

where m is the OFDM symbol index, k is the subcarrier index, S is the pilot spacing, $S_{\mathrm{p}} = \frac{m}{S} \cdot S$ S is the preceding training symbol index,$S_{\mathrm{f}} = \frac{m}{S} \cdot S$ is the following training symbol index, and ⌊. ⌋ and ⌈. ⌉ stand for the floor and ceiling operations, respectively.

3.8 Combining for detection

In the final stage, while receiving data symbols, the equalized data symbols are calculated by maximum ratio combining the N samples obtained by applying the virtual steering vectors. The effective weight vectors for CR can be obtained as,

$$\begin{aligned}
\mathbf{w}_{\mathrm{CR}} &= [\mathbf{w}_{\mathrm{V},1}, \mathbf{w}_{\mathrm{V},2}, \ldots, \mathbf{w}_{\mathrm{V},N}]\mathbf{w}_{\mathrm{MCR}} \\
&= \sum_{n=1}^{N} \left(\mathbf{w}_{\mathrm{V},n}\overline{g}_{\mathrm{V},n}\right) / \sqrt{\sum_{n=1}^{N} \left|\overline{g}_{\mathrm{V},n}\right|^2} \\
&= \sum_{n=1}^{N} \left(\overline{\Sigma}_{\mathrm{NI}}^{-1}\mathbf{h}_{\mathrm{V},n}\overline{g}_{\mathrm{V},n}\right) / \sqrt{\sum_{n=1}^{N} \left|\overline{g}_{\mathrm{V},n}\right|^2} \\
&= \mathbf{\Sigma}_{\mathrm{NI}}^{-1}\overline{\mathbf{g}} / \overline{\mathbf{g}},
\end{aligned} \tag{18}$$

where $\overline{\mathbf{g}} = \left[\overline{g}_{\mathrm{V},1}, \overline{g}_{\mathrm{V},2}, \ldots, \overline{g}_{\mathrm{V},N,}\right]^{\mathrm{T}}$. It is enough to calculate and use this weight vector $\mathbf{w}_{\mathrm{CR}}$, instead of separately applying the MRC weights on the samples obtained by the weight vectors $[\mathbf{w}_{\mathrm{V},n}]$. The equalized data symbols are then calculated as follows:

$$\hat{d} = \mathbf{w}_{\mathrm{CR}}^{\mathrm{H}}\mathbf{r}. \tag{19}$$

In Eq. (19), $\overline{\mathbf{g}}$ appears as the spatial channel estimate for the target CR transmitter. Overall, this is the zero-forcing IRC solution which maximizes the received signal power over normalized steering vectors.

4 Results and discussion

The simulations are carried out for the system setup explained in Sect. 2. The carrier frequencies of CR and PU are the same, and it is here set to 700 MHz, which is close to the upper edge of the terrestrial TV frequency band. The modulation order used by CR varies between 4QAM, 16QAM, and 64QAM. The pilot symbols are binary and have the same power level as the data symbols. The primary transmitter signal follows the DVB-T model with 16QAM modulation, 8 MHz bandwidth, and CP length of 1/8 times the useful symbol duration, i.e., 28 μs. The IFFT/FFT length is 2048 for both systems. The DVB-T and CR systems use 1705 and 1200 active subcarriers, respectively. PUs frame structure and pilots follow the DVB-T standard. Data in all signals are generated randomly. ITU-R Vehicular A channel model (about 2.5 μs delay spread) is used for the CR system. For short-range/indoor CR communication, Ricean-fading channel model would be more relevant, but the Rayleigh-fading Vehicular A model is used as worst-case model. We have also tested basic scenarios with the Ricean-fading SUI-1 model (0.9 μs delay spread) for the CR, showing slight improvements in performance. Hilly Terrain channel model (about 18 μs delay spread) is used for PU transmission. The CR receiver is assumed to have four antennas, and uncorrelated 1×4 SIMO configurations are used for both the primary signal and the CR signals.

The number of spatial channel realizations simulated in these experiments is 300–1000. The ratio of CR and PU signal power levels at the CR receiver (referred to as the signal-to-interference ratio, SIR) is varied. In the case of co-channel CR interference, the average power levels of interfering and target CRs are the same at the target receiver and the channels are independent instances of the Vehicular A model with random timing offsets, while all multi-path delays remain with the CP. The lengths of the OFDM symbol frame and silent gap for interference covariance matrix estimation are also varied (expressed in terms of CP-OFDM symbol durations). A very basic training symbol scheme is assumed for the CR: training symbols contain pilots in all active subcarriers and the spacing of training symbols is 8 OFDM symbols. Frame length is selected in such a way that training symbols appear as the first and last symbol of each frame, along with other positions. Channel estimation uses linear interpolation between the training symbols. We have tested the BS-CR link performance with SIR values of {− 10, − 20, − 30} dB using silent gap durations of {8, 16, 32} OFDM symbols (known channel case also with 128 symbols), and data block lengths of {17, 25, 33, 41} OFDM symbols.

4.1 The effect of silent gap length

This subsection analyzes the BER performance of the proposed sample covariance-based IRC process using Eqs. (10), (12), (18), and (19), considering the known channel-based process as an ideal reference. As it was explained in Sect. 3, the known channel case assumes perfect knowledge of the interference channel and it provides a theoretical

performance bound for practical IRC schemes. It uses the LMMSE solution (8) with known channel-based covariance estimate (9). Otherwise, the receiver process is the same as in the sample covariance-based scheme, thus providing a theoretically achievable bound for the practical sample covariance-based approach. Below, the known channel model is applied with PU interference only, assuming no cochannel CR interferers.

Figure 2 shows the BER performance considering both the known channel and sample covariance-based approaches in stationary case (no mobility). Here, the silent gap durations are 8, 16, 32, and 128 OFDM symbols and the data block length is 17. With zero-mobility, link performance is independent of the data block length and short block is used here mainly to reduce simulation time. It can be observed that the sample covariance-based simulation results converge to the corresponding known channel results with increasing gap length, since the covariance estimate is improved with increasing sequence length. This demonstrates that the known channel-based bound is theoretically achievable.

In Fig. 3, the BER performance of known channel and sample covariance approaches is shown considering SIR values of $\{-10, -20, -30\}$ dB. Similar to Fig. 2, the data block length is 17 and the gap duration is selected as 16 OFDM symbols. Zero-mobility case is considered also here. As seen in Fig. 3, the CR link performance of both known channel and sample covariance schemes is rather independent of the SIR.

A detailed comparison between the required SNR values of the known channel and sample covariance-based approaches for BER $= 0.01$ is provided in Table 1. As seen in the table, the required SNR values of known channel and sample covariance-based algorithms match adequately under the gap length of 128 OFDM symbols. Additionally, the numerical results clearly show that the differences in required SNR values are almost independent of the SIR while considering the SIR values of $\{-10, -20, -30\}$ dB. The SNR loss due to limited gap length is about 0.3 dB, 1 dB, 1.9 dB, and 4.4 dB for gap lengths of 128, 32, 16, and 8, respectively.

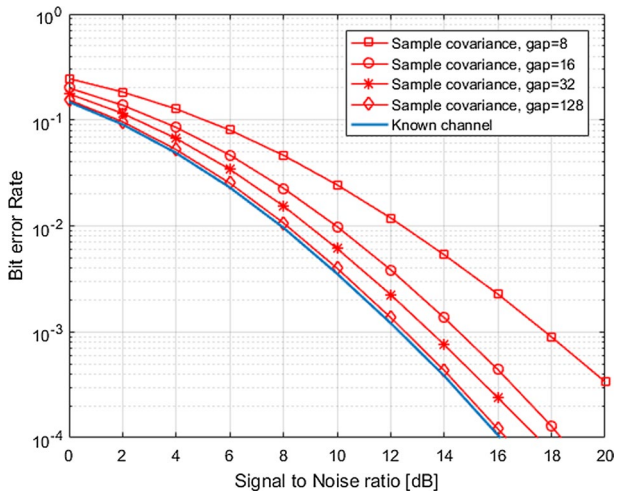

Fig. 2 Performance of QPSK BS-CR systems with known channel-based and sample covariance-based approaches for SIR $= -30$ dB considering block fading channel (no-mobility) with silent gap lengths of 8, 16, 32 and 128 symbols, and OFDM frame length of 17 symbols

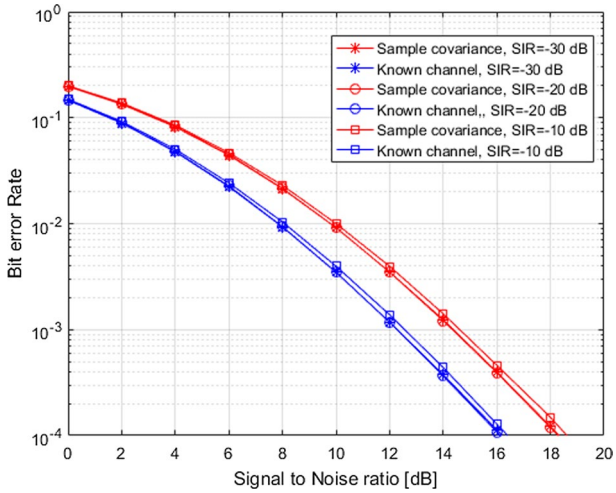

Fig. 3 Performance of QPSK BS-CR systems with known channel and sample covariance-based approaches for SIR values of {− 10, − 20, − 30} dB considering block fading channel (no-mobility) with silent gap length of 16 OFDM symbols and OFDM frame length of 17 symbols

Table 1 Required SNR values of known channel and sample covariance-based approaches for the BER = 0.01 in QPSK BS-CR systems for SIR values of {− 0, − 20, − 30} dB considering block fading channel (no-mobility) with silent gap lengths of 8, 16, 32 and 128 symbols, and OFDM frame length of 17 symbols.

Req. SNR for BER = 0.01	SIR = − 30 dB		SIR = − 20 dB		SIR = − 10 dB	
	Known Chn. (dB)	Sample Cov. (dB)	Known Chn. (dB)	Sample Cov. (dB)	Known Chn. (dB)	Sample Cov. (dB)
Gap = 8	7.9	12.3	7.9	12.3	7.9	12.2
Gap = 16	7.9	9.8	7.9	9.8	7.9	9.7
Gap = 32	7.9	8.9	7. 9	8.9	7.9	8.8
Gap = 128	8.0	8.3	8.0	8.3	8.0	8.2

4.2 Performance analysis of proposed scheme with mobility

This subsection reports the performance analysis of the proposed algorithms considering also the effects of mobility and different system parameters. It is noted that only sample covariance-based approach is considered in the following results. The results presented above still serve as ideal reference when evaluating the effects of mobility in different configurations. First we evaluate the performance with slow mobilities with and without pilot interpolation, still assuming that the interference is due to the PU only.

Figure 4 shows the impact of covariance matrix interpolation on the BS-CR link performance. Here the data block length and gap duration are fixed to 17 and 16 OFDM symbols, respectively. This choice provides performance that is no more than 1 dB from the configuration reaching 1% or 10% BER with lowest SNR, among the tested configurations with even higher overhead. We can see that covariance interpolation provides significant improvement of robustness in time-varying channels. Focusing on the 1 – 10% BER region, the performance with interpolation at 10 km/h mobility clearly exceeds the performance at 3 km/h without interpolation. However, for the 64QM case with -30 dB SIR, this is true only for BER of 10% or higher, due to the high error floor at very low

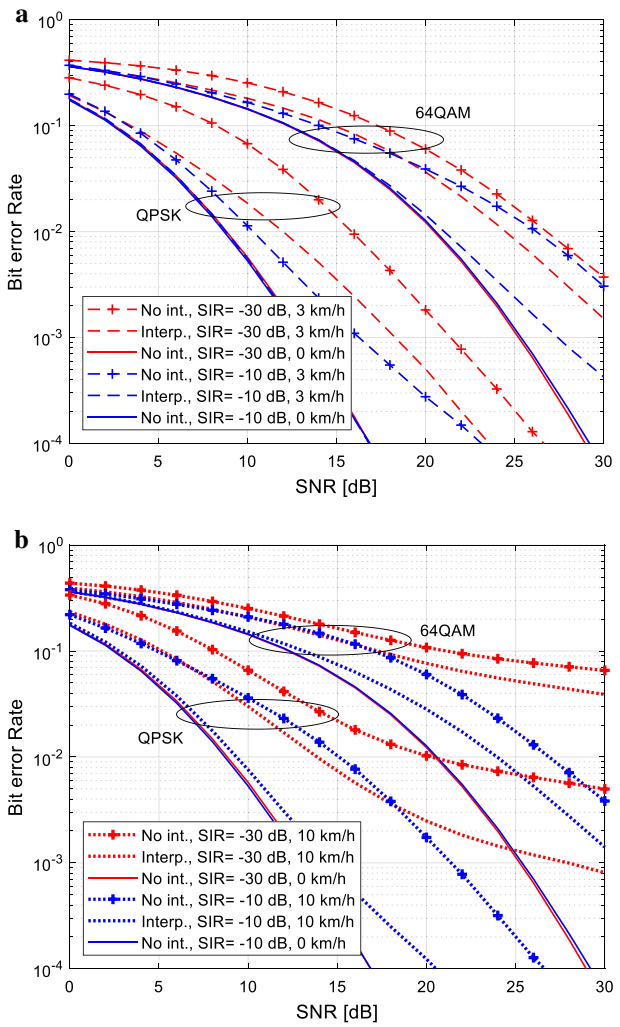

Fig. 4 Performance of QPSK and 64QAM BS-CR systems for SIR {− 10, − 30} dB with or without covariance matrix interpolation. **a** 0 and 3 km/h CR receiver mobilities. **b** 0 and 10 km/h CR receiver mobilities. Silent gap length of 16 symbols, and OFDM frame length of 17 symbols

SIR and high mobility. We can also see that with stationary channel, the performance is practically independent of the SIR. (Compared with [9], the performance is slightly improved by fine-tuning the used algorithms.)

In Fig. 5, the effect of silent gap duration is tested with 16 QAM modulation, SIR of − 20 dB, and data block length of 17. The overhead in data rate is about 58% and 44% for gap lengths of 16 and 8, respectively. The shorter gap length results in about 1.5 dB performance loss in the 1–10% range in stationary case and about 1.8–3.5 dB loss with 10 km/h mobility, compared to the gap length of 16. With 20 km/h mobility, the corresponding loss is about 2.2 dB at 10% BER, but longer gap leads to higher error floor, and the performance with shorter gap becomes better for BER below 3%.

Finally, we evaluate the link performance in the presence of co-channel CR interference, in addition to PU interference. While still assuming four antennas in the target CR receiver and − 20 dB SIR for the PU signal, also two interfering CR signals are included

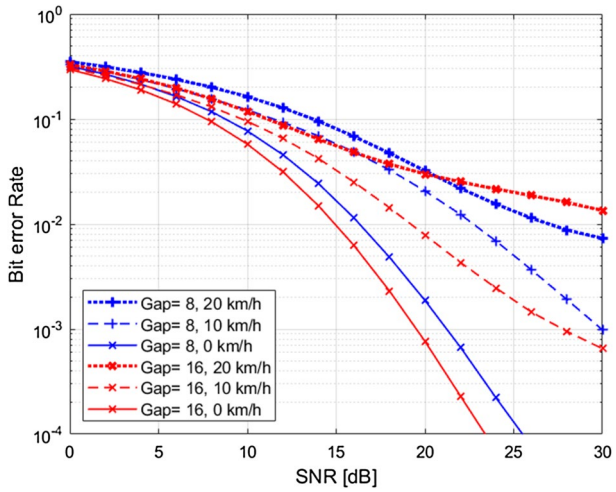

Fig. 5 Performance of QPSK and 16QAM BS-CR systems for SIR = − 20 dB with covariance matrix interpolation for CR receiver mobilities of 0, 10 km/h, and 20 km/h. Silent gap length of 8 or 16 symbols and OFDM frame length of 17 symbols

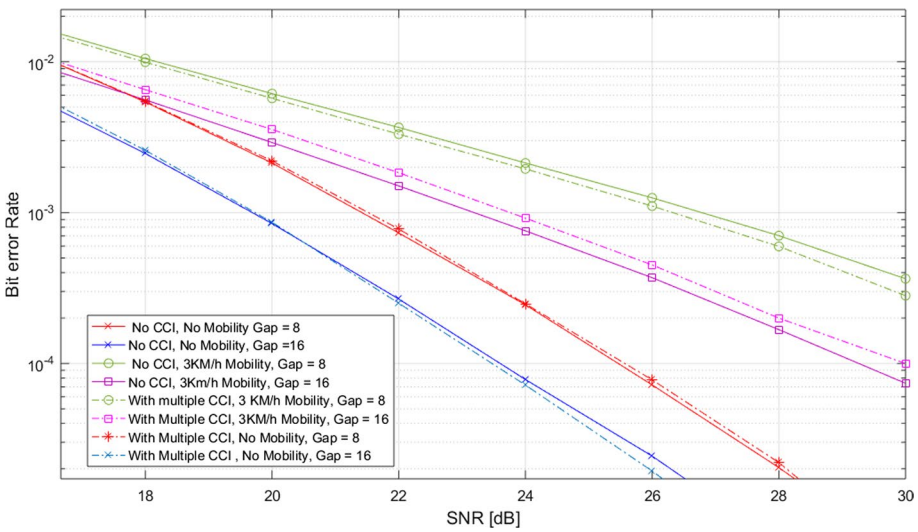

Fig. 6 Link performance in the presence of PU and two CR co-channel interferers using gap lengths of 8 and 16, mobilities of 0 and 3 km/h, 16QAM modulation in target CR link, SIR of − 20 dB for PU, and equal power levels of all CR signals

in the model. All CR signals are at the same average power level and their channels are independent instances of the Vehicular A channel model. The results are shown in Fig. 6, indicating that the impact of co-channel CRs on the target link performance is very minor.

5 Conclusion

The performance of black-space CR transmission links in the presence of strong interferences and mobility was investigated using spatial covariance interpolation between silent gaps. The interference rejection capability of IRC using multiple receive antennas

for various modulation orders under varying mobility and channel setups was studied. It was found that the IRC performs very well in the basic SIMO-type BS-CR scenario when stationary channel model is applicable, e.g., in fixed wireless broadband scenarios. However, the scheme is rather sensitive to the fading of the PU channel, e.g., due to people moving close to the CR receiver. Due to the strong interference level, the interference cancellation process is affected by relatively small errors in the covariance matrix estimate. For covariance estimation, the silent gap length in the order of 16—32 OFDM symbols provides the best performance with stationary channels, but even with 3 km/h mobility, the performance degrades greatly when considering SIR levels below -10 dB. The data block length should be of the same order or less, which leads to high overhead due to the silent gaps. Covariance interpolation was shown to greatly improve the robustness with time-varying channels, such that good link performance can be obtained with up to 20 km/h mobility at 700 MHz carrier frequency. This indicates that the proposed BS-CR scheme could be feasible at below 6 GHz frequencies with pedestrian mobilities. However, there is a significant tradeoff between link performance and overhead in data rate due to the silent gaps.

In the basic TV black-space scenario, there is only one strong TV signal present in the channel, in agreement with our assumption about the primary interference sources. DVB-T system allows also single-frequency network (SFN) operation and the use of repeaters to improve local coverage. In both cases, the primary transmissions can be seen as a single transmission, with a spatial channel that depends on the specific transmission scenario, and the proposed scheme is still applicable.

One important issue in the proposed scheme is its sensitivity to the nonlinearities of the CR receiver's analog front-end. Wide linear range is required in order to prevent nonlinear distortion from the high-power PU signal from degrading the CR link performance. This is a common issue with opportunistic CR operating in white spaces close to high-power PU channels and also with digital signal processing (DSP) intensive receiver architectures. An interesting technology in this context is advanced DSP algorithms for compensating the nonlinear effects of the receiver's analog front end [26]. On the other hand, sample covariance-based IRC may exhibit some capability to reject also the nonlinear distortion due to the strong PU signal. This remains as an important topic for future studies.

The scheme was also extended to scenarios where multiple CR systems are operating in the same region. If all CR systems are time-synchronized to the PU and they are at a relatively small distance from each other, they are also synchronized with each other, and can be handled by the IRC process as additional interference sources following the model of Eq. (3).

In future work, it is important to optimize the silent gap and data block lengths along with the modulation order to maximize throughput with given PU interference level and mobility. Lower-order modulations are more robust to errors in covariance estimation, allowing significantly lower gap and training overhead than higher order modulation. Complexity reduction of the covariance interpolation and IRC process is also an important topic for further studies. It is also worth to consider adaptation of the IRC process without silent gaps after the first one required for the initial solution. This would help to reduce the related overhead in throughput. One possible approach is to do this in a

decision-directed manner: first estimating the covariance matrix in the presence of the target signal and then cancelling its effect based on detected symbols and estimated target channel. In future studies, also the effect of antenna correlation will be taken into consideration.

Abbreviations

BER: Bit error rate; BS-CR: Black-space cognitive radio; CP-OFDM: Cyclic prefix orthogonal frequency division multiplexing; CR: Cognitive radio; dB: Decibels; DVB-T: Digital video broadcasting, terrestrial; FFT: Fast Fourier transform; IFFT: Inverse fast Fourier transform; IRC: Interference rejection canceller; LMMSE: Linear minimum mean-squared error; OFDM: Orthogonal frequency division multiplexing; QAM: Quadrature amplitude modulation; QPSK: Quadrature phase shift keying; MRC: Maximum ratio combining; MIMO: Multiple input multiple output; PU: Primary user; SFN: Single frequency network; SIR: Signal-to-interference ratio; SINR: Signal to interference and noise Ratio; SIMO: Single input multiple output; SU: Secondary user; TVWS: TV white space.

Acknowledgements

This work was supported in part by the Finnish Cultural Foundation.

Authors' contributions

The idea, analysis, simulations and writing were done by SS, with the help of SD and MR. All authors read and approved the final manuscript.

Funding

This work was supported in part by the Finnish Cultural Foundation.

Availability of data and materials

Not applicable.

Competing interests

The authors declare that they have no competing interests.

Received: 15 January 2020 Accepted: 20 October 2020
Published online: 23 November 2020

References

1. T. Yucek, H. Arslan, A survey of spectrum sensing algorithms for cognitive radio applications. IEEE Comm. Surv. Tutor. **11**(1), 116–129 (2009)
2. Y.C. Liang, A. T. Hoang Y. Zeng, R. Zhang, A review on spectrum sensing for cognitive radio: challenges and solutions, in *EURASIP Journal on Advances in Signal Processing*, pp. 1–15, January 2010.
3. S. Dikmese, S. Srinivasan, M. Shaat, F. Bader, M. Renfors, Spectrum sensing and resource allocation for multicarrier cognitive radio systems under interference and power constraints, in *EURASIP Journal on Advances in Signal Processing*, 2014:68.
4. A.M. Wyglinski et al., *Cognitive Radio Communications and Networks: Principles and Practice* (Academic Press, Cambridge, 2010)
5. Y. Selén, R. Baldemair, J. Sachs, A short feasibility study of a cognitive TV black space system, in *Proc. IEEE PIMRC 2011*, Toronto, ON, 2011, pp. 520–524.
6. A. Rico-Alvariño, C. Mosquera, Overlay spectrum reuse in a broadcast network: covering the whole grayscale of spaces, in *Proc. IEEE* DySPAN 2012, WA, 2012, pp. 479–488.
7. Z. Wei, Z. Feng, Q. Zhang, W. Li, Three regions for space-time spectrum sensing and access in cognitive radio networks. IEEE Trans. Veh. Technol. **64**(6), 2448–2462 (2015)
8. Y. Beyene, K. Ruttik, R. Jantti, Effect of secondary transmission on primary pilot carriers in overlay cognitive radios, in *Proc. CROWNCOM2013*, Washington, DC, 2013, pp. 111–116.
9. S. Srinivasan, M. Renfors Interference rejection combining for blackspace cognitive radio communications, in *Proc. Crowncom 2018*, Ghent, Belgium, pp. 200–210, Sept. 2018.
10. Srinivasan S., Renfors M. (2019) Interference rejection combining for black-space cognitive radio communications, in: eds *Cognitive Radio Oriented Wireless Networks*, I. Moerman, J. Marquez-Barja, A. Shahid, W. Liu, S. Giannoulis, X. Jiao, CROWNCOM 2018.
11. A.B. Carleial, A case where interference does not reduce capacity, in *IEEE Trans. Information Theory*, 01/1975.
12. N. Devroye, P. Mitran, V. Tarokh, Achievable rates in cognitive radio channels. IEEE Trans. Inf. Theory **52**, 1813–1827 (2006)
13. S. Verdu, *Multiuser Detection* (Cambridge University Press, Cambridge, 1998)
14. J. Winters, Optimum combining in digital mobile radio with cochannel interference, in *IEEE Trans. on Vehicular Technology*, vol 2, Issue 4, August 1984.
15. J. Liaster, J. and Reed, Interference rejection in digital wireless communication, in *IEEE Signal Processing Magazine*, vol 14, Issue 3, May 1997
16. G. Klang, On interference rejection in wireless multichannel systems, PhD Thesis, KTH, Stockholm, Sweden, 2003.

17. M.A. Beach et al, Study into the Application of Interference Cancellation Techniques, Roke Manor Research Report 72/06/R/036/U, April 2006.
18. O. Bakr, M. Johnson, R. Mudumbai, K. Ramchandran, Multi antenna interference cancellation techniques for cognitive radio applications, in *Proc. IEEE WCNC 2009*.
19. C.C. Cheng, S. Sezginer, H. Sari, Y.T. Su, Linear interference suppression with covariance mismatches in MIMO-OFDM systems. IEEE Trans. Wirel. Commun. **13**, 7086–7097 (2014).
20. S. Srinivasan, S. Dikmese, D. Menegazzo, and M. Renfors, Multi-antenna interference cancellation for black space cognitive radio communications, in *Proc.* 2015 *IEEE Globecom Workshops*, San Diego, CA, 2015, pp. 1–6
21. U. Ladebusch, C.A. Liss, Terrestrial DVB (DVB-T): a broadcast technology for stationary portable and mobile use. Proc. IEEE **94**, 183–193 (2006).
22. S. Haykin, *Adaptive Filter Theory*, 4th edn. (Prentice-Hall, New York, 2001)
23. M. Alonso et al. Spectrum occupancy and hidden node margins for cognitive radio applications in the UHF band, in: eds *Mobile Multimedia Communications. MobiMedia 2011*, Lecture Notes of the Institute for Computer Sciences, Social Informatics and Telecommunications Engineering, vol 79. L. Atzori, J. Delgado, D. Giusto (Springer, Berlin, Heidelberg, 2012)
24. C. He, Z. Peng, Q. Zeng, Y. Zeng, A novel OFDM interpolation algorithm based on comb-type pilot, in *Wireless Communications Networking and Mobile Computing 2009*. WiCom '09. 5th International Conference on, pp. 1–4, 2009.
25. L.J. Cimini, Analysis and simulation of a digital mobile channel using orthogonal frequency division multiplexing. IEEE Trans. Commun. **33**(7), 665–675 (1985)
26. M. Valkama, A. Shahed hagh ghadam, L. Anttila, M. Renfors, Advanced digital signal processing techniques for compensation of nonlinear distortion in wideband multicarrier radio receivers. IEEE Trans. Microw. Theory Tech. **54**(6), 2356–2366 (2006)

Publisher's Note